Volume 22, No 3 | International Journal of Radiation Research, July 2024

Cytotoxic effects of chloridazon-loaded alginate-chitosan nanocapsules on the 4T1 breast cancer cell line.

S. Babaei[1], D. Kahrizi[2*], N. Karimi[3,4], I. Nosratti[4], E. Arkan[5], S. Ercişli[6], M.B. Tahir[7]

[1]*Nanobiotechnology Department, Faculty of Innovative Science and Technology, Razi University, Kermanshah, Iran*
[2]*Agricultural Biotechnology Department, Faculty of Agriculture, Tarbiat Modares University, Tehran, Iran*
[3]*Nanobiotechnology Department, Faculty of Innovative Science and Technology, Razi University, Kermanshah, Iran*
[4]*Department of Agronomy and Plant Breeding, Faculty of Agriculture, Razi University, Kermanshah, Iran*
[5]*Nano Drug Delivery Research Center, Health Technology Institute, Kermanshah University of Medical Sciences, Kermanshah, Iran*
[6]*Faculty of Agriculture, Department of Horticulture, Ataturk University, 25240, Erzurum, Turkey*
[7]*Department of Physics, Khawaja Fareed University of Engineering and Information Technology, Rahim Yar Khan, Pakistan*

► ***Original article***

Corresponding author:
Danial Kahrizi, Ph.D.,
E-mail: *dkahrizi@modares.ac.ir*

Received: November 2023
Final revised: January 2024
Accepted: January 2024

Int. J. Radiat. Res., July 2024; 22(3): 739-748

DOI: 10.61186/ijrr.22.3.739

Keywords: *Alginate-Chitosan Nanocapsule, Chloridazon, Pyridazinone, Cytotoxicity.*

ABSTRACT

Background: Chloridazon belongs to the pyridazinone group of herbicides. Pyridazinone derivatives are known to have various pharmacological activities, including anti-cancer effects. Therefore, our study aimed to assess the cytotoxicity, apoptotic, anti-metastasis, and anti-angiogenesis effects of chloridazon-loaded alginate-chitosan nanocapsules on the 4T1 breast cancer cell line. ***Materials and Methods:*** The 4T1 cell line was cultured in RPMI 1640 media and treated with different concentrations of chloridazon-loaded alginate-chitosan nanocapsules. Cell viability was evaluated using the MTT assay, while cell vitality was assessed using the NR uptake assay. Apoptosis was induced and observed through acridine orange and propidium iodide staining. Furthermore, the expression levels of genes associated with metastasis (MMP-2 & MMP-9) and angiogenesis (VEGF-A) were analyzed using the RT-PCR technique. ***Results:*** The chloridazon-loaded nanocapsules displayed increased cytotoxicity on the 4T1 cell line in a dose-dependent manner. As the treatment dose increased, both cell viability and vitality decreased. The IC50 of the nanoformulation was measured as 74 µg/ml based on the dose-response curve. Additionally, the nanoformulation was found to induce apoptosis and decrease the expression levels of genes related to metastasis (MMP-2 & MMP-9) and angiogenesis (VEGF-A). Notably, the doses of 100 µg/ml and 160 µg/ml of the nanoformulation exhibited the most significant effects. ***Conclusion:*** Our findings reveal that the chloridazon-loaded alginate -chitosan nanocapsules have the potential to exert cytotoxic effects on the 4T1 breast cancer cell line.

INTRODUCTION

Drug nanoencapsulation is a promising technique that has been extensively studied in recent years. It involves enclosing drug molecules in a nano-sized carrier system. These carriers, also known as nanoparticles, can be made from various materials such as lipids, polymers, or metals. The primary objective of drug nanoencapsulation is to enhance the pharmacokinetics and pharmacodynamics of the drug. This technique offers several advantages, including protection of the drug from degradation, controlled drug release, improved drug solubility, and enhanced stability. Moreover, encapsulating drugs in a carrier enables targeted delivery to specific sites within the body and facilitates transport across physiological barriers. This approach minimizes unwanted side effects and enhances therapeutic efficacy [1-4]. Ultimately, drug nanoencapsulation holds immense potential for various applications, including cancer treatment, infectious diseases, tumor immunotherapy, and other medical conditions [5-8]. Notably, it has been extensively explored in cancer treatment due to its ability to deliver drugs specifically to tumor cells while minimizing harm to healthy tissue [9,10].

Natural polymers, such as chitosan, alginate, hyaluronic acid, and silk fibroin, show promise for drug delivery applications. These polymers are extensively investigated in nanoencapsulation due to their biocompatibility and biodegradability. Utilizing natural polymers in nanoencapsulation approaches can enhance drug solubility, stability, and controlled release [11]. Alginate, a naturally occurring

[DOI: 10.61186/ijrr.22.3.739]

polysaccharide, has excellent pH sensitivity, biocompatibility, superior gelling properties, and low toxicity, making it suitable for drug nanoencapsulation [12,13]. Another natural polymer, chitosan, is one of the most extensively studied materials for drug nanoencapsulation. It is biocompatible, biodegradable, and positively charged, allowing for interaction with negatively charged molecules. Chitosan nanoparticles have shown promising results in improving the solubility, stability, and oral bioavailability of poorly soluble drugs [14,15]. Combining alginate and chitosan through ionotropic gelation results in the formation of a gel matrix that can effectively encapsulate bioactive compounds. This interaction between the polymers leads to the formation of nano-sized particles that encapsulate the compounds. Additionally, this combination can enhance the solubility and bioavailability of poorly soluble compounds and enable controlled release [16].

Chloridazon (5-Amino-4-chloro-2- phenylpyridazin-3 (2H)-one) is a selective herbicide that is commonly used for controlling weeds in fields of vegetables [17]. Research conducted by Šiviková K *et al*. (1999) demonstrated the ability of chloridazon to interact with eukaryotic cell DNA [18]. Chloridazon belongs to the pyridazinone group of herbicides and is also known as 5-amino-4-chloro-2-phenyl-3(2H)-pyridazinone. The chemical structure of chloridazon features a substituted pyridazinone ring, which is a characteristic feature of compounds in the pyridazinone group. Specifically, in the molecular structure of chloridazon, pyridazin-3(2H)-one is substituted by an amino group at position 5, a chloro group at position 4, and a phenyl group at position 2 [19]. Pyridazinone derivatives have displayed a wide range of pharmacological activities, including antihypertensive, adrenoceptor antagonism, cardiotonic effects, anti-inflammatory properties, asthma inhibition, and anticancer activity [20]. Preclinical studies have demonstrated promising anticancer effects of pyridazinones, which act by inhibiting enzymes involved in DNA replication and transcription. These compounds have shown activity against various cancer types, including breast, lung, and colon cancer [21,22]. Novel 3(2H)-pyridazinone derivatives were designed and synthesized by Özdemir Z *et al*. (2020) and evaluated through different experimental assays to assess their preliminary in vivo toxicity and in vitro anti-proliferative effects against HCT116 cell lines. The results revealed that certain compounds exhibited promising anti-proliferative effects against HCT116 cells, either alone or in the presence of serotonin as a pro-inflammatory factor, mimicking an inflamed model in vivo of a cancer cell microenvironment [23]. Another study by I.G R *et al*. (2012) focused on a series of novel 6-aryl-2-(p-sulfamylphenyl)-pyridazin-3(2H)-ones and their anticancer activity. These novel pyridazinone derivatives showed acceptable activity against leukemia, non-small cell lung cancer, colon, central nervous system, melanoma, ovarian, and breast cancer cell lines [24].

In our study, we aimed to investigate the biological effects of nanoencapsulated chloridazon, particularly regarding its cytotoxicity, induction of apoptosis, and alteration of gene expression related to metastasis and angiogenesis in the 4T1 mouse breast cancer cell line. We utilized chloridazon-loaded alginate-chitosan nanocapsules for the treatment. Our research is the first to explore the effectiveness of chloridazon nanoencapsulation and its biological effects on breast cancer cells in an animal model utilizing the BALB/c-derived 4T1 model.

MATERIALS AND METHODS

Chemicals

Roswell Park Memorial Institute (RPMI) 1640 medium, Fetal bovine serum (FBS), and Trypsin containing Ethylenediaminetetraacetic acid (EDTA) were purchased from Gibco/Life Technologies, Inc, USA. 3 - (4,5-dimethylthiazol-2-yl) - 2,5-diphenyl tetrazolium bromide (MTT), Natural red (NR), Acridine orange (AO), Propidium iodide (PI), Dimethyl sulfoxide (DMSO), were purchased from Sigma-Aldrich, USA. Technical. Chloridazon was kindly provided as a gift by Bisetoon Kermanshah Chemical Complex, Inc., Iran.

Preparation of Chloridazon-loaded Alginate-Chitosan Nanocapsules

In this particular study, both chloridazon-loaded alginate-chitosan nanocapsules and blank alginate-chitosan nanocapsules, previously synthesized in our earlier research, were utilized. The chitosan-alginate nanocapsules were prepared through a two-step process involving the ionotropic pre-gelation of an alginate core, followed by the creation of a chitosan polyelectrolyte complex. The protocol utilized in our previous study [25] was applied. Different concentrations of chloridazon (10 µg/ml, 20 µg/ml, 40 µg/ml, 80 µg/ml, 100 µg/ml, 160 µg/ml, and 200 µg/ml) were prepared based on the drug loading percentage of nanocapsules. For the present study, blank chitosan-alginate nanocapsules (100 µg/ml) and technical chloridazon (100 µg/ml) were employed.

Cell Culture and Treatment

The 4T1 mouse breast cancer cell line was obtained from the Pasture Institute, Cell Bank of Iran (NCBI, Tehran, Iran). The 4T1 cells were cultured in 25T flasks (SPL. Pro Lab Supply Corp, USA) containing 5 ml of RPMI 1640 medium supplemented

[DOI: 10.61186/ijrr.22.3.739]

with 10% FBS. The flasks (Labotect.C200, Germany) were incubated (Memmert. ICO240, Germany) in a 5% CO^2 atmosphere at 37°C for 24 hours. After three passages, the cells were treated with varying concentrations of chloridazon-loaded nanocapsules. Additionally, technical chloridazon was used as a positive control group in all conducted tests.

Evaluation of cell viability using MTT Assay

Cell viability refers to the percentage of living cells within a given cell population. Initially, 4T1 cells (5×10^4 cells/well) were seeded into 96-well plates (SPL. Pro Lab Supply Corp, USA) containing 200 µl of growth medium. The plates were incubated at 37°C and 5% CO^2 for 24 hours. Following incubation, different concentrations of chloridazon-loaded alginate-chitosan nanocapsules (10, 20, 40, 80, 100, and 200 µg/ml) were added to each well. Blank chitosan-alginate nanocapsules (100 µg/ml) and technical chloridazon (100 µg/ml) were added to separate wells as well. Some wells remained untreated and served as negative controls. After 24 hours of cell treatment, the MTT assay was performed according to the method described by Rahmani-Kukia N *et al*. (2020) [26]. Briefly, 20 µl of MTT solution (5 mg/ml) was added to each well, and the plate was covered and incubated for 4 hours in a 5% CO2 atmosphere at 37°C. After incubation, the supernatant was removed from all wells, and 100 µl of DMSO was added to each well. The plate was then shaken for 10 minutes to dissolve the formazan crystals. Absorbance was measured at 540 nm using a microplate reader (Multiskan™ FC Microplate Photometer, Thermo Fisher Scientific, USA). The difference in viability between the control group and the treated groups was calculated, with the cell viability level of the control group set as 100%. The survival rate (%) was calculated using equation 1.

$$\text{Cell viability \%} = OD_{\text{Sample}} / OD_{\text{Control}} \times 100 \quad (1)$$

Evaluation of Cell Viability through Lysosomal Neutral Red (NR) Dye Uptake

Cell viability plays a crucial role in determining the physiological health of cells post-drug treatment. The NR assay was conducted following the same methods of preparing cell culture and treatments as the MTT assay, with the exception that NR testing utilized 20 µl of NR solution (3.3 mg/ml) added to each well, after which the plate was covered and incubated for 4 hours in a 5% CO^2 atmosphere at 37° C. Following incubation, the supernatant was removed from the wells, and 100 µl of a PBS solution containing 10% acetic acid and 40% ethanol was added to the wells and the plate was then shaken for 15 minutes. Subsequently, the absorbance at 630 nm was measured to evaluate cell vitality, and the survival rate (%) was determined using equation 1.

Assessment of Cell Apoptosis

The apoptosis test was performed based on the method described by Rahmani-Kukia N *et al*. (2018) [27], utilizing AO and PI staining. 4T1 cells were cultured in a 24-well plate (1×10^6 cells/well) and incubated at 37°C in a 5% CO^2 atmosphere for 24 hours. Subsequently, the cell cultures were treated with varying concentrations of chloridazon-loaded alginate-chitosan nanocapsules (40, 80, 100, and 160 µg/ml), followed by a 24-hour incubation at 37°C in a 5% CO^2 atmosphere. Blank chitosan-alginate nanocapsules (100 µg/ml) and technical chloridazon (100 µg/ml) were used as the positive control, while a negative control group was included. The supernatant was then removed, and the cells were washed twice with PBS. Next, the cells were stained with 10µl of AO (10 µg/ml) for 15 minutes at room temperature in the dark. Subsequently, 10µl of PI (10 µg/ml) was added to the cell pellets. Apoptosis was evaluated using fluorescent inverted microscopy (echo LAB, SM 500 FI, Italy), and the percentage of cells exhibiting apoptosis was quantified.

Analysis of metastasis and angiogenesis gene expression level using real-time PCR

To assess the metastasis rate of 4T1 cells, the expression levels of MMP-2 and MMP-9 genes, as well as the angiogenesis rate through the expression level of the VEGF-A gene, were evaluated. The HPRT gene served as the internal control for transcriptional analysis. 4T1 cells were cultured in a 6-well plate (1×10^6 cells/well) and incubated for 24 hours, followed by treatment with varying concentrations of chloridazon-loaded alginate-chitosan nanocapsules (40, 80, 100, and 160 µg/ml), blank chitosan-alginate nanocapsules (100 µg/ml), and technical chloridazon (100 µg/ml). A control group was also included. Total RNA from the treated cells was extracted using TRIzol (Sigma-Aldrich, USA) according to the manufacturer's instructions. The quality and quantity of the extracted RNA were assessed using a spectrophotometer (NanoDrop™ 8000, Thermo Fisher Scientific, USA), and the 260/280 ratio was confirmed to be 1.9. Complementary DNAs were synthesized using the cDNA synthesis kit (Easy cDNA Synthesis Kit, Parstous, IRAN) following the manufacturer's instructions. Specific primers were designed using the NCBI website and AlleleID.7 software (Premier Biosoft, USA) (Table 1). The expression levels of the target genes were determined using the StepOne Plus Real-Time PCR system (Applied Biosystems|Thermo Fisher Scientific, USA). The expression ratio of the desired genes was calculated using the ΔΔct method, as indicated by equation 2.

$$R = 2^{-\Delta\Delta ct} \quad [\Delta\Delta ct = \Delta ct_{\text{target sample}} - \Delta ct_{\text{reference sample}}] \quad (2)$$

[DOI: 10.61186/ijrr.22.3.739]

Table 1. List of designed primers.

Gene	Primer sequence	Annealing temperature (C°)
MMP-2 (104bp)	F – GGACAAGAACCAGATCACATAC R – CGTCGCTCCATACTTTTAAGG	60
MMP-9 (180bp)	F – GTGTCTGGAGATTCGACTTG R – CCTTGTTCACCTCATTTTGG	58
VEGF-A (173bp)	F – GGATCAAACCTCACCAAAGC R – GCAGGAACATTTACACGTCTG	61
HPRT (102bp)	F – CAGGACTGAAAGACTTGCTC R – AGGTCAGCAAAGAACTTATAGC	63

Statistical Analysis

All experiments were conducted in triplicate. Firstly, the data were assessed for normality. The results were analyzed using mean ± SD and one-way ANOVA for statistical analysis. The half-maximal inhibitory concentration (IC50) of chloridazon-loaded alginate-chitosan nanocapsules was determined through a non-linear regression curve-fit analysis. All analyses were conducted using GraphPad Prism ver 8.0 (San Diego, CA, USA). A confidence level of 95% was considered for all tests, and a P-value below 0.05 was deemed significant.

RESULTS

Characterization of Chloridazon-Loaded Alginate-Chitosan Nanocapsules

As previously mentioned, the chloridazon-loaded nanocapsules were synthesized in our previous study. Characterization of these nanocapsules revealed an average size of 253 nm and a polydispersity index (PDI) of 0.266. The zeta potential value obtained was -1.43 mV. In our previous study, the drug loading of the synthesized nanocapsules was found to be 14% with an encapsulation efficiency of 57%. Furthermore, our measurements demonstrated that the highest release amount (65%) occurred within the first 5 hours, followed by a stable release rate over the next 40 hours [25].

Measurement of cell viability by MTT assay

The MTT assay is a colorimetric assay used to measure cellular metabolic activity, serving as an indicator of cell viability, proliferation, and cytotoxicity. The number of viable 4T1 cells significantly decreased in a dose-dependent manner when treated with chloridazon-loaded nanocapsules at concentrations ranging from 20 to 200 µg/ml compared to the control group. Additionally, the group treated with technical chloridazon exhibited a significant difference compared to the control group ($P < 0.05$, figure 1). Conversely, the blank chitosan-alginate nanocapsules did not show significant differences in cell viability compared to the control group. Notably, the concentration of 100 µg/ml of chloridazon-loaded nanocapsules had a similar effect to that of technical chloridazon (100 µg/ml). Although the difference between these two treatment groups was not statistically significant, the data indicated that the group treated with chloridazon-loaded nanocapsules (100 µg/ml) had a lower average number of viable cells in the assay (average cell viability for technical chloridazon was 22.79 ± SD, while for the 100 µg/ml chloridazon-loaded nanocapsules was 19.89 ± SD). The concentration of 200 µg/ml of chloridazon-loaded nanocapsules had a significant effect on decreasing cell viability. The blank alginate-chitosan nanocapsules did not exhibit a significant cytotoxic effect. The IC50 index, representing the concentration of a drug causing 50% inhibition of a biological process or activity, was determined to be 74 µg/ml for the chloridazon-loaded nanocapsules, based on the dose-response curve obtained from testing the biological effect of different concentrations of the chloridazon-loaded alginate-chitosan nanocapsules on the 4T1 cell line.

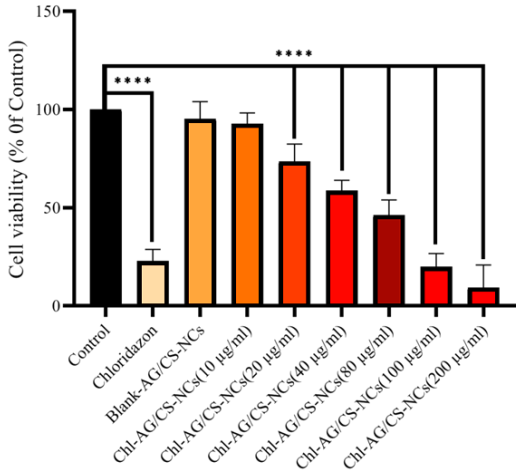

Figure 1. Measurement of cell viability by MTT assay in 4T1 cancer cells treated with different concentrations of chloridazon-loaded nanocapsules, blank nanocapsules (100 µg/ml), and technical chloridazon (100 µg/ml). The viable cell number at the 20 – 200 µg/ml concentrations of treatment chloridazon-loaded nanocapsules groups, was significantly decreased in a dose-dependent manner compared to the control group. (Blank-AG/CS- NCs: blank chitosan-alginate nanocapsules, Chl-AG/CS-NCs: chloridazon-loaded alginate-chitosan nanocapsules). The data represent the mean ± SD from three independent experiments. *P < 0.05.

Measurement of cell vitality by neutral red (NR) Assay

The vitality of 4T1 cancer cells treated with different concentrations of chloridazon-loaded alginate-chitosan nanocapsules, blank chitosan-alginate nanocapsules (100 µg/ml), and technical chloridazon (100 µg/ml) was measured using the Neutral Red (NR) assay. The results were similar to the MTT assay in this study. The control group showed a significant difference compared to the technical chloridazon ($P < 0.05$, figure 2). The concentrations of chloridazon-loaded nanocapsules (20-200 µg/ml) had a significant difference compared to the control group. The 10 µg/ml concentration of chloridazon-loaded nanocapsules also had a significant difference compared to the control group. The 200 µg/ml concentration of chloridazon-loaded

[DOI: 10.61186/ijrr.22.3.739]

nanocapsules had a more pronounced cytotoxic effect compared to the technical chloridazon. The blank chitosan-alginate nanocapsules did not exhibit a significant cytotoxic effect (P < 0.05).

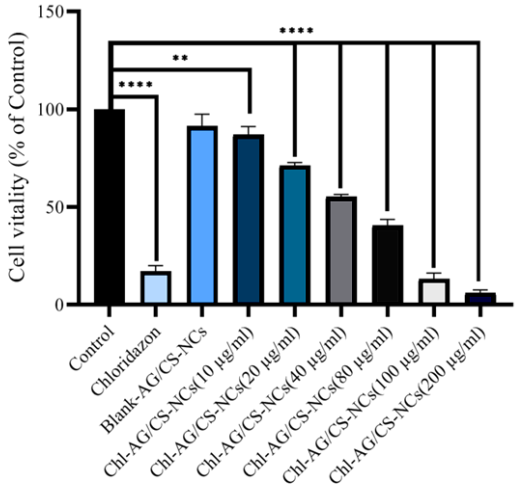

Figure 2. Measurement of cell vitality by natural red (NR) assay in 4T1 cancer cells treated with different concentrations of chloridazon-loaded nanocapsules, blank nanocapsules (100 µg/ml), and technical chloridazon (100 µg/ml). All concentrations of the treatment chloridazon-loaded nanocapsules in a dose-dependent manner significantly have a difference with the control group. The 200 µg/ml concentration of chloridazon-loaded nanocapsules had a more pronounced cytotoxic effect. (Blank-AG/CS- NCs: blank chitosan-alginate nanocapsules, Chl-AG/CS-NCs: chloridazon-loaded alginate-chitosan nanocapsules). The data represent the mean ± SD from three independent experiments. *P < 0.05.

Measurement of cell apoptosis using AO and PI

The cytotoxic effect of different concentrations of chloridazon-loaded alginate-chitosan nanocapsules and technical chloridazon on 4T1 cells was evaluated using AO and PI staining. AO stains live cells with green fluorescence, while PI stains apoptotic cells with red fluorescence. The treated 4T1 cells revealed apoptosis stages (figure 3). There was a significant difference between the control group and the chloridazon-treated groups. Additionally, there was a significant difference between the control group and all the treatment groups (P < 0.05, figure 4). However, there was no significant difference between the group treated with the technical chloridazon and those treated with the 100 µg/ml concentration of chloridazon-loaded nanocapsules. The 160 µg/ml concentration of chloridazon-loaded nanocapsules had a more pronounced effect on inducing apoptosis. The blank chitosan-alginate nanocapsules did not significantly affect apoptosis induction (P < 0.05).

Measurement of the cell metastasis and angiogenesis by real-time PCR

The RNA expression levels of MMP-2, MMP-9 genes (markers for metastasis rate), and VEGF-A gene (a marker for angiogenesis rate) in 4T1 cells treated with different concentrations of chloridazon-loaded alginate-chitosan nanocapsules were measured using real-time PCR.

The results of the MMP-2 expression level analysis showed a significant difference between the control group and all the treatment groups, except for the group treated with blank alginate-chitosan nanocapsules. However, no significant difference was observed between the concentration of 100 µg/ml of chloridazon-loaded alginate-chitosan nanocapsules and technical chloridazon (100 µg/ml) (P < 0.05, figure 5). Similar results were obtained for the analysis of MMP-9 expression levels (figure 6). When comparing the effects of the 100 µg/ml and 160 µg/ml concentrations of chloridazon-loaded alginate-chitosan nanocapsules on the RNA expression levels of MMP-2 and MMP-9 genes, no significant difference was observed (p < 0.05).

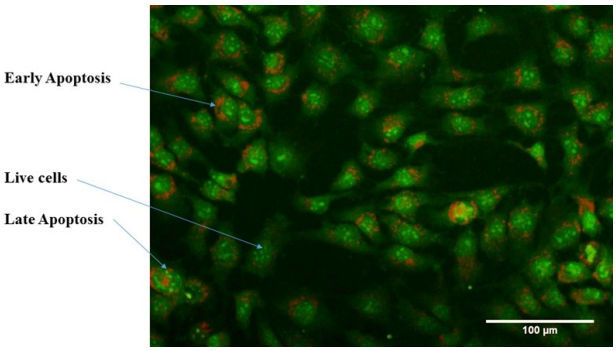

Figure 3. Fluorescent microscopic image of 4T1 cells treated with chloridazon-loaded alginate-chitosan nanocapsules (80 µg/ml). Stages of apoptosis were shown in the image.

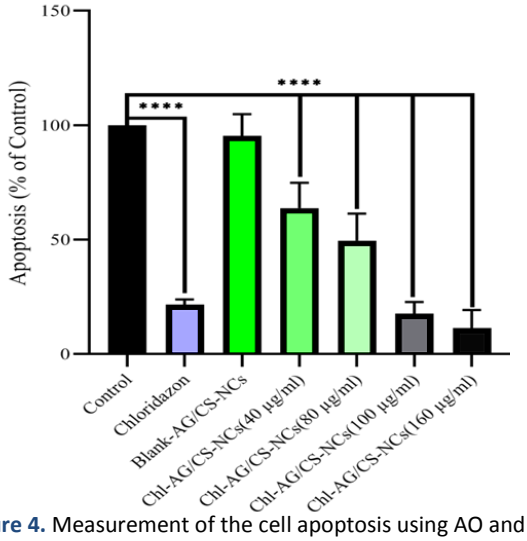

Figure 4. Measurement of the cell apoptosis using AO and PI in 4T1 cancer cells treated with different concentrations of chloridazon-loaded nanocapsules, blank nanocapsules (100 µg/ml), and technical chloridazon (100 µg/ml). There was a significant difference between the control group and all the chloridazon-loaded nanocapsules treatment groups in a dose-dependent manner. The 160 µg/ml concentration of chloridazon-loaded nanocapsules had a more pronounced effect on inducing apoptosis. (Blank-AG/CS- NCs: blank chitosan-alginate nanocapsules, Chl-AG/CS-NCs: chloridazon-loaded alginate-chitosan nanocapsules). The data represent the mean ± SD from three independent experiments. *P < 0.05.

[DOI: 10.61186/ijrr.22.3.739]

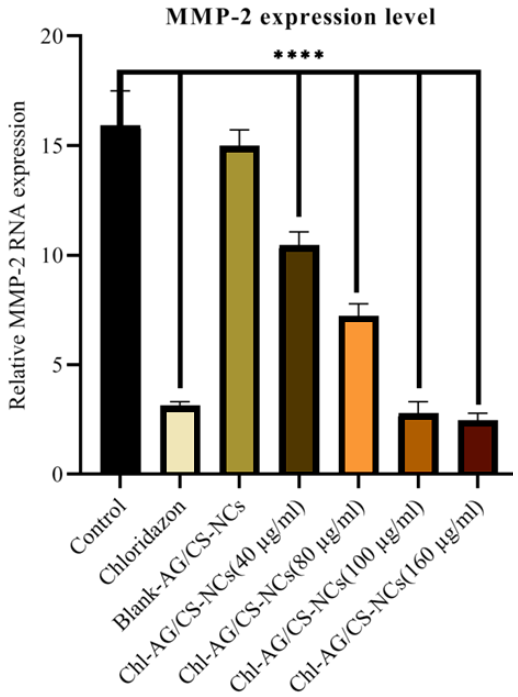

Figure 5. The mRNA expression levels of MMP-2, in the 4T1 cancer cells treated with different concentrations of chloridazon-loaded nanocapsules, blank nanocapsules (100 µg/ml), and technical chloridazon (100 µg/ml). The control group was significantly different from all the chloridazon-loaded nanocapsules treatment groups and also dose-dependent effects are evident in the treatment groups. (Blank-AG/CS- NCs: blank chitosan-alginate nanocapsules, Chl-AG/CS-NCs: chloridazon-loaded alginate-chitosan nanocapsules). The data represent the mean ± SD from three independent experiments. *P < 0.05.

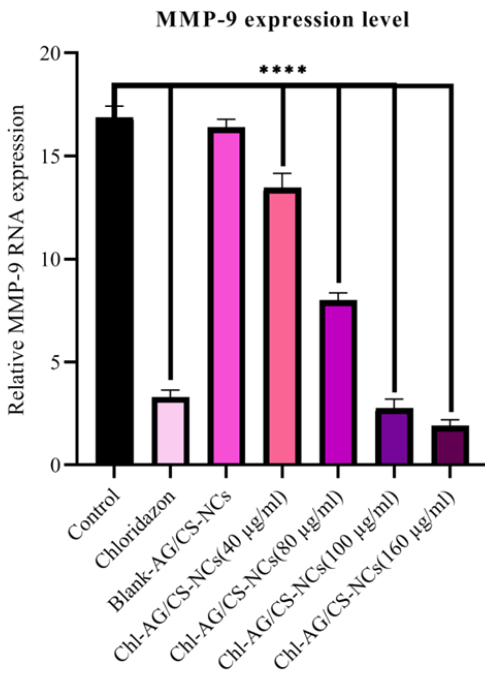

Figure 6. The mRNA expression levels of MMP-9, in the 4T1 cancer cells treated with different concentrations of chloridazon-loaded nanocapsules, blank nanocapsules (100 µg/ml), and technical chloridazon (100 µg/ml). The control group was significantly different from all the chloridazon-loaded nanocapsules treatment groups and also dose-dependent effects are evident in the treatment groups. (Blank-AG/CS- NCs: blank chitosan-alginate nanocapsules, Chl-AG/CS-NCs: chloridazon-loaded alginate-chitosan nanocapsules). The data represent the mean ± SD from three independent experiments. *P < 0.05.

In terms of VEGF-A expression level analysis, the control group showed a significant difference from all the groups treated with chloridazon-loaded nanocapsules and technical chloridazon (P < 0.05, figure 7). There was no significant difference between the groups treated with technical chloridazon and the concentrations of 100 µg/ml and 160 µg/ml of chloridazon-loaded nanocapsules. Additionally, the group treated with blank alginate-chitosan nanocapsules did not show a significant difference compared to the control group (P < 0.05).

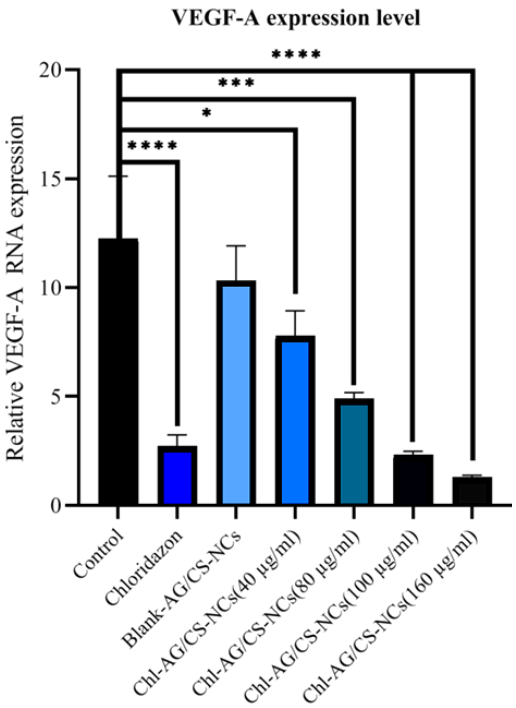

Figure 7. The mRNA expression levels of VEGF-A, in the 4T1 cancer cells treated with different concentrations of chloridazon-loaded nanocapsules, blank nanocapsules (100 µg/ml), and technical chloridazon (100 µg/ml). The control group was significantly different from all the chloridazon-loaded nanocapsules treatment groups and also dose-dependent effects are evident in the treatment groups. There was no significant difference between the groups treated with technical chloridazon and the concentrations of 100 µg/ml and 160 µg/ml of chloridazon-loaded nanocapsules. (Blank-AG/CS- NCs: blank chitosan-alginate nanocapsules, Chl-AG/CS-NCs: chloridazon-loaded alginate-chitosan nanocapsules). The data represent the mean ± SD from three independent experiments. *P < 0.05.

[DOI: 10.61186/ijrr.22.3.739]

DISCUSSION

In current research, medicinal nanocarriers composed of alginate and chitosan polymers hold promise for facilitating the treatment of various diseases. In this study, we utilized these polymers for chloridazon nanoencapsulation. The synergy of alginate with chitosan lies in the carboxylic acid groups on the surface of the alginate polymer chain, which confer negative charges to alginate. Consequently, it can electrostatically interact with positively charged molecules such as chitosan to form a gel. The formation of nanoparticles is rapid due to the spontaneous diffusion of the polymer solution in the aqueous phase, as they endeavor to avoid water molecules. Alongside the solvent diffusion from the nanoparticles, the polymer is deposited in the form of nanocapsules [16]. McMillan *et al*. (2011) indicated in their study that the shape and size of nanoparticles influence their interactions with cells, thereby impacting their distribution, toxicity, and ability to target cells [28]. Furthermore, it has been observed that nanoparticles with a size of 100 nm exhibit 2.5 times greater cellular absorption and 6 times better absorption compared to particles with a diameter of 1 µm, and 10 µm particles, respectively [29]. The average size of our synthesized chloridazon-loaded alginate-chitosan nanocapsules was 253 nm, which is a good size for nanocarriers. Additionally, PDI values close to 0.2 are generally deemed acceptable for polymer-based nanoparticles in practical applications [30]. Meanwhile, the PDI of our synthesized nanocapsules was equal to 0.266 which indicates a colloidal suspension and an acceptable homogeneous size distribution. The negative surface charge (-1.4 mV) of chloridazon-loaded nanocapsules denotes the acceptable stability of the formulated nanocapsules. The negative surface charge of the formulated nanocapsules can be attributed to a higher proportion of alginate than chitosan in their structure. This negative charge helps to mitigate accumulation and maintain the colloidal structure of the chloridazon-loaded nanocapsules. However, it is insufficient to prevent interaction with the surface of cells, which are negatively charged due to the presence of membrane phospholipids.

Our results, following prior research, corroborated the potential of alginate-chitosan nanocapsules for drug delivery and controlled release [31-34]. It is worth noting that our results, supported by the obtained data and statistical analysis, affirmed the non-toxicity of the alginate-chitosan co-polymer at the nanostructure scale on the biological activities of the 4T1 cells. This finding is consistent with numerous previous studies that underscore the biocompatible, non-toxic, and biodegradable characteristics of these polymers [35-41]. In our study, we anticipated a higher release of chloridazon during the initial hours of release (65%) due to the faster degradation of alginate compared to chitosan in the environment. As documented in our previous study, the complete release of chloridazon occurred within 40 hours [25]. This relatively rapid release of chloridazon in a neutral pH aqueous solvent can be attributed to the greater solubility of alginate compared to chitosan in an aqueous medium. Notably, chitosan exhibits its highest solubility in acidic environments [42], while alginate is highly soluble in aqueous environments [43]. In numerous studies focusing on alginate-chitosan nanocarriers, the promising potential of this type of drug carrier has been highlighted. Li. X *et al*. (2022) utilized alginate-chitosan nanocarriers for successful oral mucosal antigen delivery [44]. Similarly, in another study, Bahreini *et al*. (2014) employed chitosan nanocarriers for the delivery and controlled release of L-asparaginase enzyme protein, used in the treatment of acute lymphoblastic leukemia [45]. Consistent with previous research, our study results affirmed the effectiveness of alginate-chitosan nanocapsules for drug delivery and controlled release [46, 47].

The controlled release of chloridazon during the treatment period led to increased cytotoxic effects. The MTT assay revealed that the viability of the 4T1 cells decreased at each concentration of chloridazon-loaded nanocapsules, in accordance with the released doses during the controlled chloridazon release process, as compared to the control group (figure 1). The duration of the MTT assay treatment was 24 hours, which might have resulted in the 4T1 cells not being fully exposed to all the chloridazon loaded in the nanocapsules. Environmental conditions and the biological characteristics of the cultured cell line should also be taken into account in this context. As anticipated, and in line with the biocompatibility characteristics of alginate and chitosan polymers, the blank alginate-chitosan nanocapsules exhibited no significant cytotoxic effects. The NR assay, comparable to the MTT assay, indicated that the vitality of the 4T1 cells was dose-dependent at any concentration of the chloridazon-loaded nanocapsules (figure 2). Furthermore, an examination of the expression level of genes associated with metastasis and angiogenesis revealed a clear, dose-dependent reduction in gene expression, especially in the case of VEGF-A, with increasing concentrations of nanocapsules containing chloridazon (figure 7).

Chloridazon is a member of the pyridazinones family, which are utilized as anti-cancer, anti-tumor, and anti-inflammatory agents today [48-52]. In a study by Murineddu *et al*. (2002), the synthesis and in vitro assessment of compounds 1-Methyl-2-phenyl (1) and 1,3-dimethyl-2-phenyl (2)-substituted pyrrole (2,3-d) pyridazinones against 60 human tumor cell lines derived from 9 types of cancer cells revealed that the antitumor activities of pyridazinone-derived

[DOI: 10.61186/ijrr.22.3.739]

compounds are associated with the flatness of the pyridazinone ring. The synthesized compounds exhibited robust antitumor activity and significant cytotoxicity [53]. Another study by Gutierrez *et al*. (2019) assessed the potential anticancer properties of a new pyridazinone derivative and identified it as a potential antineoplastic agent in acute promyelocytic leukemia cells. The Pyr-1 compound demonstrated potent cytotoxicity against 22 human cancer cell lines with selective cytotoxicity against leukemia, breast, and lung cancer cell lines. Furthermore, Pyr-1 induced apoptosis in acute promyelocytic leukemia cells, as corroborated by phosphatidylserine externalization, mitochondrial depolarization, caspase - 3 activation, DNA fragmentation, and disruption of cell cycle progression. Additionally, Pyr-1 was found to induce oxidative and proteotoxic stress by stimulating the accumulation of reactive oxygen species (ROS), consequently leading to overexpression of hmox-1 mRNA and stress-related protein transcripts, along with a significant increase in polyubiquitinated proteins. The results indicated that Pyr-1 triggers cell death through the intrinsic apoptosis pathway by accumulating ROS and disrupting proteasome activity [54].

Regarding chloridazon, its nanoencapsulation was found to enhance its cytotoxic effects. When compared to the treatment of 4T1 cells with technical chloridazon (100 µg/ml), which significantly decreased cell viability in the MTT assay, the IC50 of chloridazon-loaded nanocapsules was 74 µg/ml. The potentially increased cytotoxicity could be attributed to factors such as reduced particle size, modification of particle surface properties, and enhanced drug stability. Several factors can influence the IC50 of drug-loaded nanocapsules, including the drug loading percentage, nanocapsule size, nanocapsule morphology, nanocapsule surface charge, drug dose, pharmacokinetic properties of the drug, and environmental factors affecting the release rate [55,56]. In the case of the chloridazon-loaded nanocapsules used in this study, parameters such as negative surface charge, drug loading percentage, increased bioavailability, and chloridazon release timeline appear to be among the most influential factors affecting the IC50 of the formulated nanocapsules.

In investigating the biological effects of chloridazon, three important properties of chloridazon were found to be influential in its anti-cancer effect against 4T1 cells, a trait shared with other compounds of the pyridazinone family. Firstly, chloridazon tends to interact with ds-DNA, leading to a reduction in the replication index and a delay in genomic replication. The interaction of chloridazon with DNA is dependent on the base sequence of DNA, with a greater interaction observed through the GC base sequence [18,57]. Secondly, chloridazon possesses the ability to interact with phospholipids in the outer leaflet of the cell's plasma membrane, potentially causing cell damage by affecting the phosphatidylcholines of the outer membrane [58]. Lastly, chloridazon, like many pyridazinone derivatives, exhibits a planar spatial structure [19], which contributes to its effectiveness.

There are many genetic, biochemical, physiological, and epigenetic findings related to breast cancer [59-80].

In conclusion, the results of our study shed light on key aspects, including the lack of cytotoxicity of the alginate/chitosan polymers and the high potential of the alginate-chitosan nanocapsules for the delivery and release of chloridazon. Furthermore, our experimental data suggest that chloridazon, as a member of the pyridazinone family, holds potential for pharmacological applications against breast cancer cells. Nonetheless, validation of our findings would require in vivo studies and clinical trials.

Recommendation

In the continuation of this study, we propose that expert researchers in this field explore the potential intervening effect of chloridazon-loaded alginate-chitosan nanocapsules on the outcomes of radiotherapy or chemotherapy. This investigation aims to examine how the application of these nanocapsules can influence the effectiveness and efficacy of radiotherapy or chemotherapy treatments. By delving into this aspect, researchers can gain valuable insights into the potential benefits and limitations of utilizing Chloridazon-Loaded Alginate-Chitosan Nanocapsules as a means of enhancing the outcomes of cancer treatments.

Declarations: Ethics approval and consent to participate are not applicable.

Consent for publication: Not applicable.

Availability of data and materials: The datasets analyzed during the current study are available from the corresponding author upon reasonable request.

Conflicts of Interest: The authors declare that they have no conflicts of interest.

Authors' contributions: In this study, D K served as the supervisor and was responsible for directing the experimental design. N K also played a role as the second supervisor. B S conducted the experiments and took charge of writing the draft manuscript. E A provided guidance as the advisor and actively participated in the experimental design. I N, as the second advisor, contributed to the data analysis. S E was involved in data curation and final manuscript revision. M-B T played a part in revising the final manuscript. All authors read and approved the final version of the manuscript.

REFERENCES

1. Kumari A, Singla R, Guliani A, *et al*. (2014) Nanoencapsulation for drug delivery. *EXCLI J*, ***13:*** *265-86.*

[DOI: 10.61186/ijrr.22.3.739]

2. Bhandari M, Nguyen S, Yazdani M, *et al*. (2022) The Therapeutic Benefits of Nanoencapsulation in Drug Delivery to the Anterior Segment of the Eye: A Systematic Review. *Front Pharmacol*, ***13:*** *903519.*
3. Chenthamara D, Subramaniam S, Ramakrishnan SG, *et al*. (2019) Therapeutic efficacy of nanoparticles and routes of administration. *Biomater Res*, ***23:*** *20.*
4. Patra JK, Das G, Fraceto LF, *et al*. (2018) Nano based drug delivery systems: recent developments and future prospects. *J Nanobiotechnol*, ***16:*** *71.*
5. Montané X, Bajek A, Roszkowski K, *et al*. (2020) Encapsulation for Cancer Therapy. *Molecules,* ***25(7):*** *1605.*
6. Kirtane AR, Verma M, Karandikar P, *et al*. (2021) Nanotechnology approaches for global infectious diseases. *Nat Nanotechnol,* ***16:*** *369–384.*
7. Brar B, Marwaha S, Poonia AK, *et al*. (2023) Nanotechnology: a contemporary therapeutic approach in combating infections from multidrug-resistant bacteria. *Arch Microbiol*, ***205:*** *62.*
8. Zhou L, Zou M, Xu Y, *et al*. (2022) Nano Drug Delivery System for Tumor Immunotherapy: Next-Generation Therapeutics. *Front Oncol*, ***12:*** *864301.*
9. Peer D, Karp JM, Hong S, *et al*. (2007) Nanocarriers as an emerging platform for cancer therapy. *Nat Nanotechnol*, ***2(12):*** *751-760.*
10. Brotons CA, Urueña CP, Imbuluzqueta I, *et al*. (2023) Encapsulated Phytomedicines against Cancer: Overcoming the "Valley of Death". *Int J Pharm*, ***15(4):*** *1038.*
11. Janrao C, Khopade S, Bavaskar A, *et al*. (2023) Recent advances of polymer based nanosystems in cancer management. *J Biomater Sci Polym Ed*, ***2:*** *1-62.*
12. He L, Shang Z, Liu H, *et al*. (2020) Alginate-Based Platforms for Cancer-Targeted Drug Delivery. *Biomed Res Int*, ***7:****1487259.*
13. Sosnik A (2014) Alginate Particles as Platform for Drug Delivery by the Oral Route: State-of-the-Art. *ISRN Pharm*, ***2014:*** *926157.*
14. Imam SS, Alshehri S, Ghoneim MM, *et al*. (2021) Recent Advancement in Chitosan-Based Nanoparticles for Improved Oral Bioavailability and Bioactivity of Phytochemicals: Challenges and Perspectives. *Polymers (Basel)*, ***13(22):*** *4036.*
15. Mikušová V, Mikuš P (2021) Advances in Chitosan-Based Nanoparticles for Drug Delivery. *Int J Mol Sci*, 22(17): 9652.
16. Deng S, Gigliobianco MR, Censi R, *et al*. (2020) Polymeric Nanocapsules as Nanotechnological Alternative for Drug Delivery System: Current Status, Challenges and Opportunities. *Nanomaterials (Basel)*, ***10(5):*** *847.*
17. Flores-Céspedes F, Daza-Fernández I, Villafranca-Sánchez M, *et al*. (2018) Lignin and ethylcellulose in controlled release formulations to reduce leaching of chloridazon and metribuzin in light-textured soils. *J Hazard Mater*, ***1(343):*** *227–34.*
18. Šiviková K, Dianovský J, Piešová E (1999) Chromosome Damage In Cultured Bovine Peripheral Lymphocytes Induced By Herbicide Chloridazon. *ACTA VET BRNO*, ***68:*** *105–110.*
19. National Center for Biotechnology Information. PubChem Compound Summary for CID 15546, Chloridazon. [Internet]. *PubChem*: [Retrieved December 11, 2023]. Available from: https://pubchem.ncbi.nlm.nih.gov/compound/Chloridazon.
20. Dubey S, Bhosle PA (2015) Pyridazinone: an important element of pharmacophore possessing broad spectrum of activity. *Med Chem Res*, ***24:*** *3579–3598.*
21. Gong J, Zheng Y, Wang Y, *et al*. (2018) A new compound of thiophenylated pyridazinone IMB5043 showing potent antitumor efficacy through ATM-Chk2 pathway. *PLoS One*, ***13(2):*** *e0191984.*
22. Sonker P, Singh M, Nidhar M, *et al*. (2022) Novel pyrimidopyridazine derivatives: design, synthesis, anticancer evaluation and in silico studies. *Future Med Chem*, ***14(23):*** *1693–704.*
23. Özdemir Z, Utku S, Mathew B, *et al*. (2020) Synthesis and biological evaluation of new 3(2H)-pyridazinone derivatives as non-toxic antiproliferative compounds against human colon carcinoma HCT116 cells. *J Enzyme Inhib Med Chem*, ***35(1):*** *1100-1109.*
24. IG Rathish, Javed K, Ahmad Sh, *et al*. (2012) Synthesis and evaluation of anticancer activity of some novel 6-aryl-2-(p-sulfamylphenyl)-pyridazin-3(2H)-ones. *Eur J Med Chem*, ***49:*** *304-30.*
25. Babaei S, Kahrizi D, Nosratti I, *et al*. (2022) Preparation and characterization of chloridazon-loaded alginate/chitosan nanocapsules: chloridazon - loaded alginate/chitosan nanocapsules. *Cell Mol Biol*, ***68(3):*** *34–42.*
26. Rahmani Kukia N, Abbasi A, Froushani S, *et al*. (2020) The effects of 17 Beta-Estradiol primed mesenchymal stem cells on the biology of co-cultured neutrophil. *Int Immunopharmacol*, ***84:*** *106602.*
27. Rahman Kukia N, Rasmi Y, Abbasi A, *et al*. (2018) Bioeffects of TiO2 nanoparticles on human colorectal cancer and umbilical vein endothelial cell lines. *APJCP*, ***19(10):*** *2821.*
28. McMillan J, Batrakova E (2011) Cell delivery of therapeutic nanoparticles. *Prog Mol Biol Transl Sci*, ***104:*** *563–601.*
29. Desai MP and Labhasetwar V (1997) The mechanism of uptake of biodegradable microparticles in Caco-2 cells is size dependent. *Pharm Res*, ***14:*** *1568–1573.*
30. Clarke S (2013) Development of hierarchical magnetic nanocomposite materials for biomedical applications. PhD thesis, Dublin City University. Available from: https://doras.dcu.ie/19392/
31. Chen Q, Li X, Xie Y, *et al*. (2021) Alginate-azo/chitosan nanocapsules in vitro drug delivery for hepatic carcinoma cells: UV-stimulated decomposition and drug release based on trans-to-cis isomerization. *Int J Biol Macromol*, ***30(187):*** *214-222.*
32. De Castro Jorge Silva A, Remirão MH, Lucas CG, *et al*. (2017) Effects of chitosan-coated lipid-core nanocapsules on bovine sperm cells. *Toxicol In Vitro*, ***40:*** *214-222.*
33. Shamekhi F, Tamjid E, Khajeh K (2010) Development of chitosan coated calcium-alginate nanocapsules for oral delivery of liraglutide to diabetic patients. *Int J Biol Macromol*, ***120(A):*** *460-467.*
34. Rivera MC, Pinheiro AC, Bourbon AI, *et al*. (2015) Hollow chitosan/alginate nanocapsules for bioactive compound delivery. *Int J Biol Macromol*, ***79:*** *95-102.*
35. Pamela V, Howard M, Stephen D, *et al*. (2002) Evaluation of the biocompatibility of a chitosan scaffold in mice. *J Biomed Mater Res*, ***59:*** *585-90.*
36. Kushwaha K, Dwivedi H (2018) Interfacial Phenomenon Based Biocompatible Alginate-Chitosan Nanoparticles Containing Isoniazid and Pyrazinamide. *Pharm Nanotechnol*, ***6(3):*** *209-217.*
37. Bagre AP, Jain K, Jain NK (2013) Alginate coated chitosan core shell nanoparticles for oral delivery of enoxaparin: in vitro and in vivo assessment. *Int J Pharm*, ***456(1):*** *31-40.*
38. Liu P and Zhao X (2013) Facile preparation of well-defined near-monodisperse chitosan/sodium alginate polyelectrolyte complex nanoparticles (CS/SAL NPs) via ionotropic gelification: a suitable technique for drug delivery systems. *Biotechnol J*, ***8(7):*** *847-54.*
39. Zohri M, Akbari Javar H, Gazori T, *et al*. Response Surface Methodology for Statistical Optimization of Chitosan/Alginate Nanoparticles as a Vehicle for Recombinant Human Bone Morphogenetic Protein-2 Delivery. *Int J Nanomedicine*, ***15:*** *8345-8356.*
40. Aluani D, Tzankova V, Kondeva Burdina M, *et al*. (2017) Evaluation of biocompatibility and antioxidant efficiency of chitosan-alginate nanoparticles loaded with quercetin. *Int J Biol Macromol*, 103: 771-782.
41. Takka S, Gürel A (2010) Evaluation of chitosan/alginate beads using experimental design: formulation and in vitro characterization. *AAPS PharmSciTech*, ***11(1):*** *460-6.*
42. Li Q, Dunn ET, Grandmaison EW, *et al*. (1992) Applications and Properties of Chitosan. *Bioact Compat Polym*, ***7(4):*** *370–97.*
43. Rinaudo M (2008) Main properties and current applications of some polysaccharides as biomaterials. *Polym Int*, ***57:*** *397–430.*
44. Li X, Kong X, Shi S, *et al*. (2008) Preparation of alginate coated chitosan microparticles for vaccine delivery. *BMC Biotechnol*, ***8:*** *89.*
45. Bahreini E, Aghaiypour K, Abbasalipourkabir R, *et al*. (2014) Preparation and nanoencapsulation of l-asparaginase II in chitosan-tripolyphosphate nanoparticles and in vitro release study. *Nanoscale Res Lett*, ***9(1):*** *340.*
46. Li S, Zhang H, Chen K, *et al*. (2022) Application of chitosan/alginate nanoparticle in oral drug delivery systems: prospects and challenges. *Drug Deliv*, ***29(1):*** *1142-1149.*
47. Hamman JH (2010) Chitosan Based Polyelectrolyte Complexes as Potential Carrier Materials in Drug Delivery Systems. *Marine Drugs*, ***8(4):*** *1305-1322.*
48. Sabt A, Eldehna WM, Al Warhi T, *et al*. (2020) Discovery of 3,6-disubstituted pyridazines as a novel class of anticancer agents targeting cyclin-dependent kinase 2: synthesis, biological evaluation and in silico insights. *J Enzyme Inhib Med Chem*, ***35(1):*** *1616-1630.*
49. Barberot C, Moniot A, Allart Simon I, *et al*. (2018) Synthesis and biological evaluation of pyridazinone derivatives as potential anti-inflammatory agents. *Eur J Med Chem*, ***146:*** *139-146.*
50. Ahmed MF, Santali EY, Mohi El Deen EM, *et al*. (2021) Development of pyridazine derivatives as potential EGFR inhibitors and apoptosis inducers: Design, synthesis, anticancer evaluation, and molecular modeling studies. *Bioorg Chem*, ***106:*** *104473.*
51. Singh J, Kumar V, Silakari P, *et al*. (2022) Pyridazinones: A versatile scaffold in the development of potential target-based novel anticancer agents. *J Heterocycl Chem*, ***60(6):*** *929–49.*
52. Özdemir Z, Alagöz MA, Arslan G, *et al*. (2022) Pharmacologically

[DOI: 10.61186/ijrr.22.3.739]

Active Molecules Bearing the Pyridazinone Ring as Main Scaffold. *GUHES*, ***4(2):*** *61-79.*
53. Murineddu G, Cignarella G, Chelucci G, *et al*. (2002) Synthesis and cytotoxic activities of pyrrole[23-d]pyridazin-4-one derivatives. *Chem Pharm Bull*, ***50:*** *754–765.*
54. Gutierrez DA, DeJesus RE, Contreras L, *et al*. (2019) A new pyridazinone exhibits potent cytotoxicity on human cancer cells via apoptosis and poly-ubiquitinated protein accumulation. *Cell Biol Toxicol*, ***35(6):*** *503-519.*
55. Aykul S, Martinez Hackert E (2016) Determination of half-maximal inhibitory concentration using biosensor-based protein interaction analysis. *Anal Biochem*, ***508:*** *97-103.*
56. Priani SE, Setianty TN, Aryani R, *et al*. (2021) Development of Nanocapsules Containing Cytotoxic Agents: A Review. *J Farmasi Galenika*, ***7(2):*** *151-165.*
57. Ahmadia F, Jamalia N, Jahangard Yektaa S, *et al*. (2011) The experimental and theoretical QM/MM study of interaction of chloridazon herbicide with ds-DNA. *Spectrochimica Acta Part A*, ***79:*** *1004–1012.*
58. Suwalsky M, Benites M, Villena F, *et al*. The organochlorine herbicide chloridazon interacts with cell membranes. *CBP Part C, 120: 29–35.*
59. Zhou T, Zhou M, Tong C & Zhuo M (2022). Cauliflower bioactive compound sulforaphane inhibits breast cancer development by suppressing NF-κB /MMP-9 signaling pathway expression: Suppressing NF-κB /MMP-9 signaling with sulforaphane. *Cellular and Molecular Biology,* ***68(4)****, 134–143. https://doi.org/10.14715/cmb/2022.68.4.17.*
60. Cheng H, Chen L, Fang Z, Wan Q, Du Z, Ma N, Guo G & Lu W (2022). The effect of miR-138 on the proliferation and apoptosis of breast cancer cells through the NF-κB/VEGF signaling pathway: Effect of miR-138 on breast cancer cells. *Cellular and Molecular Biology,* ***68(2)****, 132–137. https://doi.org/10.14715/cmb/2022.68.2.19.*
61. Zhang Y, Yuan J, Zhang Q, Yan J, Ju S & Yang Y (2022). Nano-lipid Contrast Agent Combined with Ultrasound-Guided SGB in Nursing Treatment of Lymphedema after Breast Cancer Surgery: Nano-lipid Contrast Agent Combined with Ultrasound-Guided SGB. *Cellular and Molecular Biology,* ***68(3)****, 189–201. https://doi.org/10.14715/cmb/2022.68.3.22.*
62. Lin J, Ding Q, Zhang G & Yin X (2022). Study on PI3k gene expression in breast cancer samples and its association with clinical factors and patient survival. *Cellular and Molecular Biology,* ***67(4)****, 321–327. https://doi.org/10.14715/cmb/2021.67.4.36.*
63. Wang D, Wang C, Sun L, Lu X, Shi J, Chen J & Zhang X (2022). MiR-143-3p Increases the Radiosensitivity of Breast Cancer Cells Through FGF1. *Cellular and Molecular Biology,* ***67(5)****, 256–262. https://doi.org/10.14715/cmb/2021.67.5.35.*
64. Xin L & Zhiyuan X (2022). Evaluating serum level of granulocyte, macrophage and granulocyte-macrophage colony-stimulating factors in patients with breast tumor: Serum level of G-CSF, M-CSF, and GM-CSF in breast tumor. *Cellular and Molecular Biology,* ***68(5)****, 146–152. https://doi.org/10.14715/cmb/2022.68.5.20.*
65. Lin R, Guan Z, Zhou Q, Zhong J, Zheng C & Zhang Z (2022). Effects of 7,12-Dimethylbenz(a)anthracene on Apoptosis of Breast Cancer Cells through Regulating Expressions of FasL and Bcl-2. *Cellular and Molecular Biology,* ***68(1)****, 201–208. https://doi.org/10.14715/cmb/2022.68.1.24.*
66. Majed SO (2022). RNA Sequencing-Based Total RNA Profiling; The Oncogenic MiR-191 Identification as a Novel Biomarker for Breast Cancer. *Cellular and Molecular Biology,* ***68(1)****, 177–191. https://doi.org/10.14715/cmb/2022.68.1.22.*
67. Çetin İdil & Topçul M (2022). Investigation of the Effects of the Endogenous Cannabinoid Anandamide on Luminal A Breast Cancer Cell Line MCF-7: Effects of the Endogenous Cannabinoid. *Cellular and Molecular Biology,* ***68(4)****, 129–133. https://doi.org/10.14715/cmb/2022.68.4.16.*
68. Chang C, Shang Y, Gao Y, Shang M, Wang L & Li H (2022). Clinical features, treatment, and prognosis of 16 breast cancer patients with ocular metastases. *Cellular and Molecular Biology,* ***67(5)****, 363–370. https://doi.org/10.14715/cmb/2021.67.5.49.*
69. Wen R, Lin H, Li X, Lai X & Yang F (2022). The Regulatory Mechanism of EpCAM N-Glycosylation-Mediated MAPK and PI3K/Akt Pathways on Epithelial-Mesenchymal Transition in Breast Cancer Cells: EpCAM N-Glycosylation and PI3K/Akt Pathways on Breast Cancer Cells. *Cellular and Molecular Biology,* ***68(5)****, 192–201. https://doi.org/10.14715/cmb/2022.68.5.26.*
70. Cheng H, Chen L, Fang Z, Wan Q, Du Z, Ma N, Guo G & Lu W (2022). STIM2 promotes the invasion and metastasis of breast cancer cells through the NFAT1/TGF-β1 pathway. *Cellular and Molecular Biology,* ***67(6)****, 55–61. https://doi.org/10.14715/cmb/2021.67.6.8.*
71. Li X, Fu H, Li P, L, Y, Li W & Zhu F (2022). Nano Carbon Tracing-based Treatment of Breast Cancer Lymphadenectomy and Nursing Intervention of Postoperative Lymphedema. *Cellular and Molecular Biology,* ***68(3)****, 304–313. https://doi.org/10.14715/cmb/2022.68.3.33.*
72. Yang Y, Jiao Y, Mohammadi MR. Post-translational modifications of proteins in tumor immunotherapy and their potential as immunotherapeutic targets. *Cell Mol Biomed Rep 2023 Feb 25. doi: 10.55705/cmbr.2023.378480.1091.*
73. Ali Salman R. Prevalence of women breast cancer. *Cell Mol Biomed Rep 2023 Mar 20. doi: 10.55705/cmbr.2023.384467.1095.*
74. Kanwal N, Al Samarrai OR, Al-Zaidi HM, Mirzaei AR, Heidari MJ. Comprehensive analysis of microRNA (miRNA) in cancer cells. *Cell Mol Biomed Rep 2023 Jun 1;****3(2):****89-97. doi: 10.55705/cmbr.2022.364591.1070*
75. Li X and Mohammadi MR. Combined Diagnostic Efficacy of Red Blood Cell Distribution Width (RDW), Prealbumin (PA), Platelet-to-Lymphocyte Ratio (PLR), and Carcinoembryonic Antigen (CEA) as Biomarkers in the Diagnosis of Colorectal Cancer. *Cell Mol Biomed Rep 2023 Jun 1;****3(2):****98-106. doi: 10.55705/cmbr.2023.374804.1088.*
76. Alsaedy HK, Mirzaei AR, Alhashimi RA. Investigating the structure and function of Long Non-Coding RNA (LncRNA) and its role in cancer. *Cell Mol Biomed Rep 2022 Dec 1;****2(4):****245-53. doi: 10.55705/cmbr.2022.360799.1062.*
77. Alavi M, Rai M, Martinez F, Kahrizi D, Khan H, Rose Alencar De Menezes I, Douglas Melo Coutinho H, Costa JG. The efficiency of metal, metal oxide, and metalloid nanoparticles against cancer cells and bacterial pathogens: different mechanisms of action. *Cell Mol Biomed Rep 2022 Mar 1;****2(1)****:10-21. doi: 10.55705/cmbr.2022.147090.1023.*
78. Alhashimi RA, Mirzaei A, Alsaedy H. Molecular and clinical analysis of genes involved in gastric cancer. Cell Mol Biomed Rep. 2021;1 (3):138-46. Alhashimi, R. A., Mirzaei, A., Alsaedy, H. Molecular and clinical analysis of genes involved in gastric cancer. *Cell Mol Biomed Rep 2021;* ***1(3):*** *138-146. doi: 10.55705/cmbr.2021.355860.1056.*
79. Tourang M, Fang L, Zhong Y, Suthar RC. Association between Human Endogenous Retrovirus K gene expression and breast cancer. Cellular, Molecular and Biomedical Reports. 2021 Apr 1;1(1):7-13. Tourang, M., Fang, L., Zhong, Y., Suthar, R. Association between Human Endogenous Retrovirus K gene expression and breast cancer. *Cell Mol Biomed Rep 2021;* ***1(1):*** *7-13. doi: 10.55705/cmbr.2021.138810.1008.*
80. Bilal I, Xie S, Elburki MS, Aziziaram Z, Ahmed SM, Jalal Balaky ST. Cytotoxic effect of diferuloylmethane, a derivative of turmeric on different human glioblastoma cell lines. *Cell Mol Biomed Rep 2021 Apr 1;****1(1):****14-22. doi: 10.55705/cmbr.2021.138815.1004.*

[DOI: 10.61186/ijrr.22.3.739]